

# The Reaction $pp \rightarrow pp\eta$ and the eta-Nucleon and Nucleon-Nucleon Interactions

M.T. Peña<sup>1,2</sup>, H. Garcilazo<sup>1,3</sup> and D.O. Riska<sup>4</sup>

<sup>1</sup> *Centro de Física das Interações Fundamentais, 1096 Lisboa, Portugal*

<sup>2</sup> *Departamento de Física, Instituto Superior Técnico, 1096 Lisboa, Portugal*

<sup>3</sup> *Escuela Superior de Física e Matemáticas, 07738 México Distrito Federal, Mexico*

<sup>4</sup> *Department of Physics, 00014 University of Helsinki, Finland*

## Abstract

The  $\pi$ ,  $\eta$  and  $\rho$  exchange contributions to the cross-section for the reaction  $pp \rightarrow pp\eta$  near threshold are calculated, with a phenomenological description of the intermediate S11 (N(1535)) resonance for all exchange mechanisms. The final state interaction in the  $pp$  system is described by realistic nucleon-nucleon interaction models. The sensitivity of the results to the phenomenological models for the  $\eta$ -nucleon transition amplitude and the nucleon-nucleon interaction is explored. The  $\eta$  exchange mechanism is found to play a dominant role. The off-shell behavior of the  $\eta N \rightarrow \eta N$  amplitude within the  $\eta$ -exchange amplitude leads to a result significantly different from that obtained with the constant scattering length approximation. The two-nucleon amplitudes that are associated with the short range components of the nucleon-nucleon interaction contribute significantly to the cross section.

## I. INTRODUCTION

The experimental program at electron and hadron beam facilities as MAMI, GRAAL, COSY, CELSIUS and SATURNE has brought considerable interest for a better theoretic-

cal understanding of the  $\eta$ -nucleon interaction and the reaction mechanisms for  $\eta$  meson production. The recent experimental results on the total cross section and the angular distributions for the reaction  $pp \rightarrow pp\eta$  very near threshold [1–4] are very instructive in this regard, especially as the angular independence of the cross section in the very near threshold region reveals that the  $\eta$ -meson is produced by a pure  $S$ -wave mechanism.

A considerable number of studies of the reaction mechanisms for  $S$ -wave  $\eta$ -production in  $pp$  collisions have been carried out. In most of these pion-exchange between the protons followed by excitation of an intermediate virtual  $N(1535)$  resonance (Fig.1) has been invoked to describe the reaction mechanism and the empirical cross section [5–7]. We here consider several additional contributions to the production amplitude besides those hitherto considered. The set of reaction amplitudes considered here are illustrated by the diagrams in Fig.2. These represent the one-nucleon term (Fig. 2a), the  $\eta$ - (Fig. 2b) and  $\pi$ - (Fig. 2c) rescattering terms, and finally the amplitudes implied by the short-range two-nucleon amplitudes which have their origin in the small components of the nucleon spinors (Fig. 2d). The "blobs" in Figs.2b and 2c represent the full scattering series for the meson-nucleon transition amplitudes.

The present study addresses the following 4 main issues:

1) The sensitivity of the calculated cross-section to the off-energy-shell  $\eta N$  scattering transition matrix. This is motivated by the example of the  $\eta d$  system, for which the  $\eta d$  scattering length and the correlated existence and position of a quasibound  $\eta NN$  state depend sensitively on the off-shell behavior of the  $\eta N$  amplitude.

2) The contributions to the cross-section of the non-resonant two-nucleon amplitudes that are implied by the short range components of the two-nucleon interactions. In the case of the analogous pion production reaction  $pp \rightarrow pp\pi^0$  these contributions, as derived from realistic nucleon-nucleon interaction models, are much larger than the resonance contributions [8].

3) The relative weight of the  $\pi$ ,  $\rho$  and  $\eta$  exchange mechanisms. Even in the case of a weak  $\eta NN$  coupling strength, the present calculation confirms the result of ref. [9], which found the  $\eta$  exchange mechanism to be the dominant one. As for the magnitude of the  $\rho$ -meson

exchange contribution, which is somewhat uncertain, here it is found to be non-negligible, if the quark model is used to determine the  $\rho NN(1535)$  transition coupling.

4) The dependence of the calculated cross section on the short range part of the NN interaction. This is expected to be large for processes as the present one, for which the effective momentum transfer between the nucleons is large.

A comment on the uncertainty in the magnitude of the  $\eta$  rescattering process is relevant here: this uncertainty by itself motivates the present calculation, which attempts to narrow it by taking advantage of the new experimental information on the  $pp \rightarrow pp\eta$  reaction. The ambiguity is due to the uncertain value of the  $\eta pp$  coupling constant,  $g_{\eta NN}$ , which is needed for the  $\eta$  production vertex in the process illustrated Fig. 2b. The realistic phenomenological NN interaction models are not sufficiently selective of its value, which they only constrain into the wide range between  $g_{\eta NN}^2/4\pi = 0.25$  and  $g_{\eta NN}^2/4\pi = 7$ , set by the Nijmegen [11] and one of the BONN [12] potential models respectively. Presumably, only extensions of these models for energies above the meson production threshold will show more dependence on the  $\eta NN$  coupling. More ambitious attempts to calculate this coupling constant by QCD sum rule methods are so far even less constraining [13].

The uncertainties that arise from the meson exchange description that is illustrated in Fig.1 mainly derive from the lack of knowledge of the heavy-meson-nucleon-N(1535) transition couplings, which cannot be determined experimentally, as this resonance lies below the threshold for decay into vector mesons and nucleons. In contrast, the sub-process scattering amplitudes indicated by the blobs in Fig. 2b and 2c have been empirically determined in [10,14,15].

The decomposition into partial waves  $\tau_\ell^j(s)$  of the complete unitary series of the complete unitary  $\eta N \rightarrow \eta N$  transition amplitude, along with the  $\pi N \rightarrow \eta N$  transition amplitude, was derived recently by Batinić *et al.* [10,14], who made a fit to all the available data on the reactions  $\pi N \rightarrow \pi N$  and  $\pi N \rightarrow \eta N$ . In ref. [15] fits were made along similar lines to the empirical data for the reactions  $\pi N \rightarrow \pi N$ ,  $\pi N \rightarrow \eta N$ ,  $\gamma N \rightarrow \pi N$  and  $\gamma N \rightarrow \eta N$  in the energy range of about 100 MeV below and above the  $\eta$  production threshold. Another

example of such work, but restricted to the  $\pi N \rightarrow \eta N$  amplitude, is given in ref. [16]. The model of refs. [10,14] has subsequently been tested in a calculation of the cross section for the reactions  $np \rightarrow d\eta$  [17] and  $\pi d \rightarrow \eta NN$  [18]. The successful description of the differential cross-section for the latter reaction, as measured at several energies [19], shows the quality of the off-energy-shell features of this model. This justifies the use of it for the "blob" in Fig. 2b. For comparison, we used also the more recent models of the second work in ref. [15].

The uncertainty range associated with the contributions that are associated with the short-range components of the nucleon-nucleon interaction is determined by the uncertainty range of the latter. That in the end turns out to be rather modest, however, as it is constrained by the requirement on the interaction models of a good description of  $pp$  scattering data. These uncertainties are therefore far less decisive than the uncertainty in the two-nucleon contributions that are associated with the excitation of intermediate  $N(1535)$  resonances by heavy-meson exchange between the nucleons (Fig. 1). The uncertainty in these amplitudes is due, besides to the uncertainty in the  $\eta NN$  coupling constant, to the very uncertain values of the heavy-meson- $N(1535)$ - $N$  couplings, as mentioned above. Thus e.g. the suggestion that  $\rho$ -meson exchange excitation of the intermediate  $N(1535)$  is completely model dependent [20].

This paper is divided into 5 sections. In section 2 we describe the amplitudes that are assumed to contribute significantly to the cross-section. In subsection 2.a the single nucleon amplitude is described. In subsection 2.b a description of the  $\pi$  and  $\eta$  exchange contributions follows. Subsection 2.c contains a description of the short-range exchange amplitudes that are associated with the nucleon-nucleon interaction. Subsection 2.d describes the  $\rho$ -exchange matrix elements. In section 3 details on the calculation are given. The numerical results for the cross section are given in section 4. Finally, section 5 contains a summarizing discussion.

## II. THE $\eta$ - PRODUCTION MECHANISMS

### A. The single nucleon amplitude

The phenomenologically satisfactory Gell-Mann-Oakes-Renner relations [21] suggest that the octet of light pseudoscalar mesons,  $\pi, K, \eta$ , are the Goldstone bosons of the broken approximate chiral symmetry of QCD. Chiral symmetry combined with  $SU(3)_F$  symmetry, then requires that the coupling of  $\eta$ -mesons to hadrons take the form

$$\mathcal{L} = -\frac{1}{f_\eta} \partial_\mu \eta A_\mu^8, \quad (1)$$

where  $A_\mu^8$  is the eight component of the axial vector current density of the hadron and  $f_\eta$  is the  $\eta$ -meson decay constant. The empirical value of  $f_\eta$  is very close to that of the pion decay constant ( $\sim 93$  MeV). Production of  $\eta$  mesons in  $S$ -waves in nuclear reactions is then governed by the axial charge operator  $A_0^8$ .

The  $i=1,2$  components of the axial charge operator are known to have significant two-nucleon components, which are implied by the nucleon-nucleon interaction [22,23]. These give a large contribution to the cross section for the reaction  $pp \rightarrow pp\pi^0$  near threshold [24]. As the difference between  $A_0^\pm$  and  $A_0^8$  only is due to the difference between  $\lambda_\pm$  and  $\lambda_8$ , it follows from (1) and the Goldberger-Treiman relation that the pseudovector  $\eta NN$  coupling constant should take the value

$$f_{\eta NN} = \frac{g_A}{2\sqrt{3}} \frac{m_\eta}{f_\eta} \simeq 2.11. \quad (2)$$

Here  $g_A$  is the axial coupling constant of the nucleon ( $g_A=1.24$ ). For the corresponding pseudoscalar coupling constant  $g_{\eta NN} = 2(m_p/m_\eta)f_{\eta NN}$  one then obtains the value 7.23, which is only slightly larger than the value 6.14, which is employed in the Bonn B model for the nucleon-nucleon interaction [12]. As shown below such a large value for the  $\eta NN$  coupling constant would not allow a satisfactory description of the experimental cross section for  $\eta$ -meson production in  $pp$  collisions. Only if the coupling constant is reduced to about a third of this value, which is the value that has been used in phenomenological descriptions of eta photoproduction [25], does a satisfactory description become possible. This indicates

that large  $SU(3)_F$  breaking corrections play a significant role in the chiral Lagrangian (1) in the case of the heavier members of the pseudoscalar octet [13]. Indeed, if in (2)  $m_\eta$  were replaced by the pion mass, as strict  $SU(3)$  symmetry would require, the desired smaller value for  $g_{\eta NN}$  would be obtained.

From (1) it follows that the amplitude for production of an  $S$  – wave  $\eta$ –meson from a single (off-shell) nucleon may be written as

$$T^{imp} = if_{\eta NN} \frac{\omega_\eta}{m_\eta} \frac{\vec{\sigma} \cdot (\vec{p}'_1 + \vec{p}_1)}{2m_p} \delta(\vec{p}'_2 - \vec{p}_2) + (1 \leftrightarrow 2). \quad (3)$$

Here  $m_\eta$  and  $m_p$  are the masses of the  $\eta$ –meson and the proton respectively,  $\omega_\eta$  is the energy of the  $\eta$ –meson, and  $\vec{p}_i$  and  $\vec{p}'_i$  ( $i = 1, 2$ ) are the initial and final nucleon momenta.

### B. The $\pi N \rightarrow \eta N$ and $\eta N \rightarrow \eta N$ transitions and the rescattering amplitudes

The explicit form of the amplitude for a transition  $aN \rightarrow bN$ , where  $a$  and  $b$  represent the initial and final mesons, may then be expressed in terms of Lorentz invariant amplitudes  $A$  and  $B$  as

$$t_{aN \rightarrow bN}^\pm = -A^\pm(s, t, u) + \frac{1}{2}(q_a + q_b)B^\pm(s, t, u), \quad (4)$$

where  $q_a$  and  $q_b$  are the 4-momenta of mesons  $a$  and  $b$  respectively and  $s, t$  and  $u$  are the three invariant (Mandelstam) kinematical variables.

For the  $\pi N \rightarrow \eta N$  and  $\eta N \rightarrow \eta N$  scattering amplitudes we employ the variable-mass isobar model described in [18,26]. In this model the spin- $\frac{1}{2}$  and spin- $\frac{3}{2}$  resonances are given a mass parameter that is set equal to  $\sqrt{s}$ , the invariant mass of the system. The meson-nucleon-isobar couplings are given expressions appropriate for scattering in states with the orbital angular momentum  $\ell_\pm = j \pm \frac{1}{2}$ .

The explicit form of the transition amplitude becomes then

$$t_{aN \rightarrow bN} = f_0^{1/2}(s)(\not{P} + \sqrt{s}) + f_1^{1/2}(s)(\not{P} - \sqrt{s}) \\ + f_1^{3/2}(s)(\not{P} + \sqrt{s}) \left[ -q_a \cdot q_b + \frac{\not{q}_a \not{q}_b}{3} + \frac{2P \cdot q_a \not{P} \cdot q_b}{3s} - \frac{P \cdot q_a \not{q}_b - \not{q}_a P \cdot q_b}{3\sqrt{s}} \right]$$

$$+f_2^{3/2}(s)(P - \sqrt{s})[-q_a \cdot q_b + \frac{\not{q}_a \not{q}_b}{3} + \frac{2P \cdot q_a P \cdot q_b}{3s} + \frac{P \cdot q_a \not{q}_b - \not{q}_a P \cdot q_b}{3\sqrt{s}}], \quad (5)$$

where  $s = P^2$ , and  $P$  is the total four-momentum of the meson-nucleon subsystem.

As shown in refs. [18] and [26], the matrix elements  $\bar{u}_2(\vec{p}'_2)t_{aN \rightarrow bN}u_2(\vec{p}_2)$  in the two-body c.m. frame are such that the functions  $f_\ell^j(s)$  are directly related to the phenomenological partial-wave elastic amplitudes in the case  $a = b$  and to the partial-wave transition amplitudes when  $a \neq b$ . Note that Eq. (5) is generally valid also when any of the four particles in the  $\pi N \rightarrow \eta N$  amplitude are off-mass-shell.

The  $\eta N \rightarrow \eta N$  and  $\pi N \rightarrow \eta N$  partial-wave transition amplitudes for the  $S_{11}$ ,  $P_{11}$ ,  $P_{13}$ , and  $D_{13}$  channels were taken from Batinić *et al.* [10,14]. To study the sensitivity of the results to this input we also included the  $\eta N \rightarrow \eta N$  transition amplitudes given in ref. [15]. The  $\pi N \rightarrow \pi N$  partial-wave amplitudes for the  $S_{11}$ ,  $S_{31}$ ,  $P_{11}$ ,  $P_{31}$ ,  $P_{13}$ ,  $P_{33}$ ,  $D_{13}$ , and  $D_{33}$  channels were taken from ref. [27]. For the  $\eta$  and  $\pi$  exchange processes the meson amplitudes were restricted to the dominant  $S$  waves.

For the S-wave meson production amplitudes in the elastic case  $a=b$  one has (see e.g. ref. [28])

$$[A(s) - (\sqrt{s} - m_N)B(s)] = \frac{16\pi s^2}{(\sqrt{s} + M)^2 - m_\eta^2} f_0(\sqrt{s}), \quad (6)$$

with

$$A(s) = -B(s)(m_N + \sqrt{s}). \quad (7)$$

At the physical threshold,  $\sqrt{s} = m_N + m_\eta$ , the  $\eta N \rightarrow \eta N$  strength to be included in the construction of the  $\eta$  exchange amplitude that corresponds to the diagram 2.b becomes proportional to the scattering length  $a_0 = f_0(m_N + m_\eta)$ :

$$A((m_N + m_\eta)^2) - m_\eta B((m_N + m_\eta)^2) = 4\pi \left(1 + \frac{m_\eta}{m_N}\right) a_0. \quad (8)$$

As in the present model the loop integration for the final-state interaction runs over the available energy for the  $\eta N$  isobar, it is natural to define an energy dependent strength as

$$\lambda_1^\eta(s) = \frac{m_\eta}{2}[A(s) - (\sqrt{s} - m_N)B(s)], \quad (9)$$

to be inserted into the expression for the rescattering diagram. The latter then becomes

$$T^\eta = i \frac{g_{\eta NN}}{2m_N} \frac{8\pi\lambda_1^\eta(s)}{m_\eta} \frac{\vec{\sigma}^2 \cdot \vec{k}}{m_\eta^2 + \vec{k}^2 - \omega_k^2} f(\vec{k}^2) + (1 \leftrightarrow 2). \quad (10)$$

Here  $(\vec{k}, \omega_k)$  is the 4-momentum of the exchanged  $\eta$  meson emitted from a nucleon of initial and final three-momentum  $p_i$  and  $p'_i$  ( $\vec{k} = \vec{p}_2 - \vec{p}'_2$  and  $\omega_k = \frac{\vec{k}_2 \cdot (\vec{p}_2 + \vec{p}'_2)}{2m_N}$ ). In the calculations, the  $\eta$ -nucleon invariant mass  $s$  is obtained by subtracting the energy of the spectator nucleon from the total energy of the NN $\eta$  system. The phenomenological form factor  $f$  that dampens out high values of the exchanged momentum is parametrized as in the Bonn B potential model [12]:

$$f(\vec{k}^2) = \left( \frac{\Lambda_\eta^2 - m_\eta^2}{\Lambda_\eta^2 + \vec{k}^2} \right). \quad (11)$$

Here the  $\eta$  cut-off mass is  $\Lambda_\eta = 1.5$  GeV.

Analogously, the  $\pi$  exchange diagram takes the form

$$T^\pi = i \frac{g_{\pi NN}}{2m_N} \frac{8\pi\lambda_1^\pi(s)}{m_\pi} \frac{\vec{\sigma}^2 \cdot \vec{k}}{m_\pi^2 + \vec{k}^2 - \omega_k^2} f(\vec{k}^2) + (1 \leftrightarrow 2), \quad (12)$$

where  $\lambda_1^\pi$  is given by an equation analogous to Eq. 9, but in which the kinematic factors of Eq. 6 are defined by

$$A(s) - (\sqrt{s} - m_N)B(s) = 4\pi \frac{2\sqrt{s}}{\sqrt{(E_1 + m_N)}\sqrt{(E_2 + m_N)}} f_0(\sqrt{s}), \quad (13)$$

with the nucleon energies given by

$$E_1 = \frac{s + m_N^2 - m_\pi^2}{2W}, \quad (14)$$

$$E_2 = \frac{s + m_N^2 - m_\eta^2}{2W}. \quad (15)$$

The relative sign between  $\lambda^\eta$  and  $\lambda^\pi$  is not fixed by unitarity [9]. The  $SU(3)$  flavor symmetric quark model gives a negative sign for it [29]. As shown below in Section 3 the influence of this sign on the total cross-section of the  $pp \rightarrow \eta pp$  is not significant because of the small effect of the pion-rescattering diagram.



### C. Short-range exchange contributions

The contributions to the axial exchange charge operator that is associated with the short-range components of the nucleon-nucleon interaction have been derived in refs. [22,24]. These contributions are derived as the nonrelativistic limit of the nonsingular part of the axial current 5-point function with external leg couplings. In the case of non-derivative couplings such terms only arise from the negative energy poles in the nucleon propagator and are therefore commonly illustrated by the nucleon-antinucleon “pair currents” Feynman diagrams in Fig.2d. The ultimate reason for the appearance of these terms is the Poincaré invariance of the 5-point functions [30].

Because of the derivative pseudovector coupling for both the  $\pi$  and the  $\eta$ , no such two-nucleon operators contribute to the  $\eta$  production operator in the reaction  $pp \rightarrow pp\eta$ , which would be directly associated with the  $\pi$ - and  $\eta$ - exchange components of the nucleon-nucleon interaction. The isospin independent effective scalar and vector exchange components of the nucleon-nucleon interaction do however give rise to two-nucleon meson production operators. A key point is that these operators are completely determined by the interaction model, and involve no parameters that are not already present in the NN interaction, besides the overall  $\eta$ -nucleon coupling.

The isospin independent scalar exchange contribution to the two-nucleon  $\eta$ -production amplitude may moreover be derived directly, without reference to the 5-point function, in the following way. Consider the isospin independent scalar exchange component of the nucleon-nucleon interaction, which is proportional to the Fermi invariant “ $S$ ”. To second order in  $v/c$ , this interaction takes the form

$$v_S^+(r)S = v_S^+(r) \left( 1 - \frac{\vec{p}^2}{m_N^2} \right) - \frac{1}{2m_N^2} \frac{\partial v_S^+}{r \partial r} \vec{S} \cdot \vec{L}, \quad (16)$$

where  $v_S^+(r)$  is a scalar function. The  $\vec{p}^2/m^2$  term in the spin-independent part of this interaction may be combined with the kinetic energy term in the nuclear Hamiltonian, by replacing the nucleon mass by the effective “mass operator”

$$m^*(r) = m_N \left[ 1 + \frac{v_S^+(r)}{m_N} \right]. \quad (17)$$

To first order in  $v_S^+(r)$ , the scalar component of the nucleon-nucleon interaction therefore implies the following two-body ‘‘correction’’ to the single nucleon  $\eta$  production operator:

$$T_2(S) = \frac{v_S^+(r)}{m_N} T_1(S) + (1 \rightarrow 2). \quad (18)$$

Here the spin-operator in  $T_1(S)$  is implicitly assumed to be that of nucleon 1 of the interacting pair of nucleons. This operator coincides in form with the scalar exchange operator derived in Refs. [22,23]. The corresponding momentum space expression is

$$T_2(S) = -i f_{\eta NN} \frac{\omega_\eta}{m_\eta} \frac{v_S^+(k_2)}{m_N} \vec{\sigma}^1 \cdot \vec{v}_1 + (1 \leftrightarrow 2). \quad (19)$$

Here  $v_S^+(k)$  is the Fourier transform of the scalar potential  $v_S^+(r)$  and  $\vec{v}_1 = (\vec{p}_1 + \vec{p}_1')/2m_N$ . This operator is completely determined by the nucleon-nucleon interaction model. Note that because the volume integral of the scalar exchange interaction is attractive in all realistic nucleon-nucleon potentials, this exchange current contribution implies an enhancement of the cross section over the value given by the single nucleon pion production mechanism.

The expression for the isospin-independent vector exchange contribution to the axial charge operator as derived from the 5-point function has been given in Refs. [22,23]. This leads to the following amplitude for  $\eta$ -meson production:

$$T_2(V^+) = -i \frac{f_{\eta NN}}{m_\eta} \frac{v_V^+(k_2)}{m_N} \left( \vec{\sigma}^1 \cdot \vec{v}_2 + \frac{i}{2m_N} \vec{\sigma}^1 \times \vec{\sigma}^2 \cdot \vec{k}_2 \right) + (1 \leftrightarrow 2). \quad (20)$$

Here  $v_V^+(k)$  is the isospin independent vector component of the nucleon-nucleon interaction.

The corresponding contribution to the  $\eta$ -meson production amplitude that is associated with the isospin part of the vector exchange component of the nucleon-nucleon interaction is

$$T_2(V^-) = -i \frac{f_{\eta NN}}{m_\eta} \frac{v_V^-(k_2)}{m_N} \left( \vec{\sigma}^1 \cdot \vec{v}_2 + \frac{i}{2m_N} \vec{\sigma}^1 \times \vec{\sigma}^2 \cdot \vec{k}_2 \right) \vec{\tau}^1 \cdot \vec{\tau}^2 + (1 \leftrightarrow 2). \quad (21)$$

This term is numerically less important than the previous one that is associated with the isospin independent vector exchange interaction, because the latter interaction is by far the stronger in all realistic nucleon-nucleon interaction models.

### D. The $N(1535)$ resonance and $\rho$ -meson exchange

Above the contribution from virtual intermediate  $N(1535)$  resonances, that are excited by  $\pi$  exchange between the two protons, was incorporated into the scattering amplitude factor  $\lambda_1^\pi(s)$  (12). Virtual intermediate  $N(1520)$  resonances may, however, also be excited (or de-excited) by  $\rho$ -meson exchange (Fig. 1). It has in fact been suggested in ref. [20] that  $\rho$ -meson exchange gives a much larger contribution to the  $\eta$ -meson production amplitude than  $\pi$  exchange. This argument was based on a comparison of photoproduction amplitudes, which, however, do not make any allowance for the mass of the  $\rho$ -meson.

To derive this  $\rho$ -meson exchange amplitude, we employ the transition Lagrangians

$$\mathcal{L}_{\eta NN(1535)} = i \frac{f_{\eta NN^*}^{(1535)}}{m_\eta} \bar{\psi}(1535) \gamma_\mu \partial_\mu \eta \psi + h.c., \quad (22)$$

$$\mathcal{L}_{\rho NN(1535)} = i g_{\rho NN^*}^{(1535)} \bar{\psi}(1535) \gamma_5 [\gamma_\mu - \frac{m^* + m_N}{m_\rho^2} \partial_\mu] \vec{\tau} \cdot \vec{\rho}_\mu \psi + h.c.. \quad (23)$$

Here  $m^*$  denotes the mass of the  $N(1535)$ ,  $m_\rho$  the mass of the  $\rho$ -meson and  $m_N$  the nucleon mass.

The expressions for the two  $\rho$ -meson exchange amplitudes, which corresponds to the two Feynman diagrams in Fig. 1 are, respectively,

$$T_1(\rho) = i \frac{f_{\eta NN^*}^{(1535)}}{m_\eta} g_{\rho NN} g_{\rho NN^*}^{(1535)} \frac{\omega_\eta}{2m_N} \frac{\vec{\tau}^1 \cdot \vec{\tau}^2}{m_\rho^2 + k_2^2} f(k_2) \frac{\vec{\sigma}^1 \cdot \vec{k}_2 - i(1 + \kappa_\rho)(\vec{\sigma}^1 \times \vec{\sigma}^2) \cdot \vec{k}_2}{m^* - i\Gamma_r/2 - m_N - \omega_\eta}, \quad (24)$$

and

$$T_2(\rho) = i \frac{f_{\eta NN^*}^{(1535)}}{m_\eta} g_{\rho NN} g_{\rho NN^*}^{(1535)} \frac{\omega_\eta}{2m_N} \frac{\vec{\tau}^1 \cdot \vec{\tau}^2}{m_\rho^2 + k_2^2} f(k_2) \frac{\vec{\sigma}^1 \cdot \vec{k}_2 - i(1 + \kappa_\rho)(\vec{\sigma}^1 \times \vec{\sigma}^2) \cdot \vec{k}_2}{m^* - i\Gamma_r/2 - m_N + \omega_\eta/2}. \quad (25)$$

Here  $g_{\rho NN}$  is the  $\rho NN$  vector coupling constant and  $\kappa_\rho$  is the ratio of the corresponding tensor to vector coupling constants. The coupling constant  $g_{\rho NN^*}^{(1535)}$  is that for the  $\rho NN(1535)$  transition coupling and  $f_{\eta NN^*}^{(1535)}$  is that for the  $\eta NN(1535)$  transition coupling. The resonance width is denoted  $\Gamma_r$  respectively.

The  $\eta NN^*(1535)$  coupling constant may be determined directly from the decay width for  $N(1535) \rightarrow N\eta$ . This gives the value  $f_{\eta NN^*}^{(1535)} = 1.7$  [8]. The  $\rho NN(1535)$  transition coupling constant  $g_{\rho NN^*}^{(1535)}$  cannot be determined in the same way, as the  $N(1535)$  lies below the threshold for  $N\rho$  decay.

For the determination of the  $\rho NN(1535)$  coupling constant we invoke the static quark model, which relates the resonance transition coupling constants to the  $\rho NN$  coupling constant  $g_{\rho NN}$ . Employment of the schematic covariant 3-quark model for the baryons of ref. [31], which reproduces the empirical baryon spectrum up to  $\sim 1700$  MeV satisfactorily, leads the following relation [32]:

$$g_{\rho NN^*}^{(1535)} = -\frac{\sqrt{2}}{9} \frac{m_\rho^2}{\omega m_q} e^{-k^2/6\omega^2} g_{\rho NN}. \quad (26)$$

Here  $m_q$  is the constituent quark mass and  $\omega$  is an oscillator parameter for the orbital wave functions, the value of which is  $\omega = 311$  MeV. In this expression  $\vec{k}$  is the momentum of the virtual  $\rho$ -meson. If it is set to 0, which is motivated by the fact that the  $\rho$ -meson is not far off shell, the relation (26) gives the value  $g_{\rho NN^*}^{(1535)} = -0.88g_{\rho NN}$ , with  $m_q = 340$  MeV.

### III. CROSS-SECTION AND DISTORTION IN THE NUCLEON-NUCLEON STATES

The total cross section for the reaction  $pp \rightarrow pp\eta$  may be expressed in the following form after integration over the delta function for conservation of total four-momentum, if relativistic three-particle phase-space coordinates are employed:

$$\sigma_{Tlab}[\mu b] = 10^4 (\hbar c)^2 \frac{m_N^2}{4p_0 E_{p_0}} \frac{m_N^2}{4\pi^3} \int_0^{q_{max}} q^2 dq \frac{k'}{\omega_q W'} |\langle \psi_{p_f}^- | M(q) | \psi_{p_0}^+ \rangle|^2. \quad (27)$$

Here the amplitude  $M(q)$  is given in units of  $\text{MeV}^{-3}$  and contains the symmetrization factor  $\sqrt{2}$  along with the spin average factor  $1/4$ . The initial on-shell relative nucleon-nucleon momentum is  $p_0 = m_N T_{lab}/2$  and the CM energy is  $W = \sqrt{4m_N^2 + 2m_N T_{lab}}$ . The maximal  $\eta$  momentum is

$$q_{max} = \frac{1}{2W} \sqrt{(W^2 - 4m_N^2 - m_\eta)^2 - 16m_N^2 m_\eta^2}. \quad (28)$$

The final relative nucleon-nucleon three-momentum in the three particle CM system is denoted  $p_f$ . Upon boosting to the NN rest frame  $p_f$  becomes  $k'$  (which does not differ much from  $p_f$  for small eta momentum  $q$ ). Furthermore  $W'^2 = 4(m_N^2 + k'^2) = W^2 + m_\eta^2 + 2W\omega_q$  is the corresponding energy squared, and  $\omega_q$  is the energy of the emitted  $\eta$ -meson:  $\omega_q = \sqrt{q^2 + m_\eta^2}$ . The matrix elements of the operators derived in section 2,

$$M = T^{imp} + T^\eta + T^\pi + T_2(S) + T_2(V), \quad (29)$$

were calculated in momentum space, which allows the non-local terms in the operators, and the energy dependence arising in the propagators of the exchanged mesons, to be handled without approximation. In principle one has to use the amplitude distorted by the initial and final state interactions described by the nucleon-nucleon  $T$  matrix in the expression for the cross section:

$$\langle \psi_{p_f}^- | M | \psi_{p_0}^+ \rangle = \langle \psi_{p_f}^- | T^{imp} + T^\eta + T^\pi + T_2(S) + T_2(V) | \psi_{p_0}^+ \rangle, \quad (30)$$

with

$$\langle k | \psi_{p_0}^+ \rangle = \frac{\delta(k - p_0)}{k^2} + \frac{\langle k | T(E_{p_0}) | p_0 \rangle}{E_{p_0} - E_k + i\epsilon}, \quad (31)$$

and

$$\langle \psi_{p_f}^- | k \rangle = \frac{\delta(k - p_f)}{k^2} + \frac{\langle p_f | T(E_{p_f}) | k \rangle}{E_{p_f} - E_k + i\epsilon}. \quad (32)$$

We have employed the Bonn and Paris potentials to calculate the nucleon-nucleon  $T$ -matrix in the final  $^1S_0$  nucleon-nucleon state. The poor knowledge on the form of the

potential above the pion production threshold ( 300 MeV) makes the issue of the distortion in the initial  ${}^3P_0$  state is more problematic ( the threshold for  $\eta$  production is 1258 MeV). Instead of extrapolating the potentials mentioned above to that region, in the absence of a more realistic extension, for the initial state we used the model of ref. [33], as done in ref. [9]. This reference gives the ratio of distortion in final and initial states to distortion in final state only, as defined by state distortion factors,

$$f_{ISI} = \frac{\int_0^{q_{max}} q^2 dq \frac{k'}{\omega_q W'} | \langle \psi_{p_f}^- | M | \psi_{p_0}^+ \rangle |^2}{\int_0^{q_{max}} q^2 dq \frac{k'}{\omega_q W'} | \langle \psi_{p_f}^- | M | \phi_{p_0}^+ \rangle |^2}, \quad (33)$$

to be 0.3, a value that will be used here. The function  $\phi_{p_0}^+$  in equation (33) denotes a plane-wave for the initial state. The fact that the reduction factor is constant can be explained by the flat behavior of the NN T-matrix at high energies [34]. This effect by the initial state interaction cannot be discarded if one wants to extract information on the poorly known value of the  $g_{\eta NN}^2/4\pi$  coupling constant.

#### IV. NUMERICAL RESULTS

In Fig. 3 the calculated cross section for the  $pp \rightarrow pp\eta$  reaction as obtained from the  $\eta$  exchange amplitude, that is represented by the diagram in Fig.2 b, is shown. The empirical values in this and in the following figures are those given in ref. [2,3]. The solid curve in Fig 3 gives the result that is obtained with the off-shell  $\eta N \rightarrow \eta N$  amplitude with energy dependence. The dash-dot-dotted curve gives the corresponding result obtained in turn with an energy independent amplitude, of constant strength fixed at the physical threshold by the scattering length. The comparison in Fig. 3 shows that the scattering length approximation gives rise to an overestimate of a factor of 6 of the calculated cross section. This striking overestimate indicates that the choice in ref. [35], of using the real part of this scattering length to determine the interaction strength is unrealistic.

The  $\eta$ -exchange result was calculated with the value  $g_{\eta NN}^2/4\pi = 0.4$  for the  $\eta$ -nucleon coupling constant. This is the value that was obtained by a fit to experimental  $\eta$  photoproduction data in ref. [25]. By scaling up the results to correspond to the one order

of magnitude larger coupling constant value that is consistent with the Bonn potential we find complete agreement with the calculation of ref. [9], where the same phenomenological  $\eta N \rightarrow \eta N$  amplitude was used.

Fig. 3 also illustrates that there is a positive interference between the one-nucleon term and the  $\eta$ -exchange diagrams as shown by the short-dashed curve. Once the interference term is taken into account, the emerging result is close to the result of the  $\eta$ -exchange diagram alone, if calculated with a constant strength fixed by the scattering length (dash-dotted line).

In Fig. 4 we show the effect of including the contribution of the pion exchange mechanism, when it is added to the sum of the contributions of single nucleon and  $\eta$ -rescattering diagram (dot-dashed line). The  $\pi$  exchange contribution amounts to a  $\sim 15\%$  increase, if the relative sign between the  $\pi$  and  $\eta$  exchange amplitudes is taken to be positive. In Fig. 4 the short-dashed curve has the same meaning as in Fig. 3. The full line represents the result of including in addition the  $\rho$ -exchange contribution.

In Fig. 5 we show the effect on the calculated cross section when the contributions of the short range exchange mechanisms that are associated with the nucleon-nucleon interaction model are added to the previously considered contributions. In Fig. 5 the short-dashed line refers to the cross section that corresponds to the impulse + rescattering diagrams as in the previous figures, and the short-dot-dashed line to the impulse + rescattering + short-range amplitudes. The addition to the impulse and rescattering diagrams of the short-range amplitudes that are associated with the isospin independent scalar (" $\sigma$ ") and vector (" $\omega$ ") exchange components of the nucleon-nucleon interaction implies a cross section that is 9 times larger than before. The  $\pi$  exchange diagram, when added to the impulse+rescattering+short-range amplitudes (dotted line) pushes the cross-section even higher, although some cancellations which occur between the short-range amplitudes and the  $\pi$ -exchange reduce the effect of the last one from 15%, as in Fig. 4, to only 5%. The short-range mechanisms also interplay with the  $\rho$ -exchange contribution, lessening its net effect, which nevertheless remains non-negligible (solid line). If, however, the ratio between

the  $\rho$ NN and the  $\rho$ NN(1535) coupling constants is taken the same as the ratio of the  $\pi$ NN and the  $\pi$ NN(1535) coupling constants ( $\approx 0.18$ ) the  $\rho$ -exchange contribution becomes negligible so that the final result cannot be distinguished from the dotted line. We consider the results obtained for the  $\rho$ -exchange with a quark model based  $\rho$ NN(1535) coupling constant to represent an upper bound for the  $\rho$  contribution. The calculated results shown in Figures 3-5 were obtained by using the Bonn B potential [12] along with the  $\eta$ N scattering model of reference [10].

To show the sensitivity of the calculated cross section values to the nucleon-nucleon potential model, we in Fig. 6 compare the effects of two different NN interactions (Paris [36]: dashed lines and Bonn B [12]: solid lines) to describe the final state, displaying the uncertainty band originated by the different short-range behavior of the NN interaction. In ref. [15] five different models for the  $\eta N \rightarrow \eta N$  transition were given. In Fig. 6 the results are shown for the Bonn B and the Paris NN potentials when model A of the second reference in [15] is used to describe the  $\eta N - \eta N$  transition as well as when the model of reference [10] is used. As to the other models for the amplitude considered in ref. [15], we have verified that models B and C fail to describe the  $pp \rightarrow pp\eta$  process. Coincidentally or not, these models correspond to a larger data set and give a poorer overall fit to the meson-nucleon amplitudes considered in that work. It is worth mentioning that according to [15] a worse description for the  $\gamma N \rightarrow \pi N$  transition is given by models B and C. As for model D of the same reference, we have checked that the corresponding results for the  $pp \rightarrow pp\eta$  reaction are close to those obtained with model A, and lie in the middle of the two uncertainty regions in Fig. 6, defined by the two border lines relative to the same NN potential model.

## V. CONCLUSIONS

The present investigation suggests the following main conclusions:

- 1) The cross section of the reaction  $pp \rightarrow pp\eta$  in the energy region near the threshold for the  $\eta$ -production is very sensitive to the off-energy-shell  $\eta$ N scattering transition ma-



trix. This sensitivity allows discrimination between extant phenomenological models for  $\eta N$  scattering. The same sensitivity is observed in the  $\eta d$  interaction, more specifically in the magnitude of the  $\eta d$  scattering length and the correlated existence and position of an  $\eta NN$  quasibound state [17].

2) The non-resonant two-nucleon amplitudes, the presence of which is implied by the short range components of the two-nucleon interaction, give significant contributions to the cross section of the reaction. The situation is in this sense similar to the case of the corresponding reaction  $pp \rightarrow pp\pi^0$ . These contributions, as derived from realistic nucleon-nucleon interaction models, are moreover much larger than the resonance contribution.

3) The contribution of the  $\pi$  exchange mechanism does not dominate over that due to  $\eta$  exchange - not even in the case of a very small  $\eta NN$  coupling. In ref. [9] one of the same phenomenological models for  $\eta N \rightarrow \eta N$  scattering ([10]) that were considered in this work was employed in a calculation of the cross section for  $\eta$  production in proton-proton collisions. When the present calculation was done with the same restricted input, the results agreed with that in ref. [9], and thus confirm the finding of that reference as to the dominance of the  $\eta$ -rescattering amplitude. The small importance of the  $\pi$ -exchange rescattering diagram relative to the  $\eta$ -exchange lessens the importance of the problem of the relative sign between the  $\eta N \rightarrow \eta N$  and  $\eta N \rightarrow \pi N$  amplitudes, which is not fixed by unitarity.

4) Only with a value for the  $\eta NN$  coupling constant considerably smaller than those used in the earlier realistic nucleon-nucleon potentials is it possible to obtain a satisfactory description of the cross section of this reaction with the present model. Here the same value for the coupling constant was used as in the analysis of  $\eta$  photoproduction data in ref. [25].

5) The  $\rho$ -exchange contribution is significant if the  $\rho NN(1535)$  coupling constant obtained in the constituent quark model is employed.

6) The effect of the nucleon-nucleon interactions in the final and in the initial states are important. In the numerical calculations the large reduction from the initial state interaction may appear masked as it may be partially compensated by the effect of using a constant strength for the  $\eta N \rightarrow \eta N$  transitions. The latter procedure was found to represent a poor

approximation, once final and initial state interactions are fully included.

### **ACKNOWLEDGMENTS**

D. O. R. thanks Dr. L. Tiator for instructive discussions. This work was supported in part by COFAA-IPN (México) and by Fundação para a Ciência e a Tecnologia, MCT (Portugal) under contracts PRAXIS XXI/BCC/18975/98 and PRAXIS/P/FIS/10031/1998 and in part by the Academy of Finland by grants No. 43982 and 44903.

## REFERENCES

- [1] A.M. Bergdolt et al., Phys. Rev. **D48**, R2969 (1993)
- [2] H. Calén et al., Phys. Lett. **B366**, 39 (1996)
- [3] H. Calén et al., Phys. Lett. **B458**, 190 (1999)
- [4] J. Smyrski and P. Wüstner, Annual Report, Forschungszentrum Jülich, 39 (1998)
- [5] C. Wilkin, "Approaches to Threshold Meson Production", Proceedings of the *International Conference Baryons '98*, World Scientific, 505 (1999).
- [6] E. Gedalin, A. Moalem and L. Razdolskaya, Nucl. Phys. **A650**, 471 (1999)
- [7] V. Bernard, N. Kaiser and U.-G. Meissner, Eur. J. Phys. **A4**, 259 (1999)
- [8] M. T. Peña, D. O. Riska, and A. Stadler, Phys. Rev. C 60, 045201 (1999)
- [9] M. Batinić, A. Švarc and T.-S. H. Lee, Physica Scripta **56**, 321 (1997)
- [10] M. Batinić, I. Šlaus, A. Švarc, and B. M. K. Nefkens, Phys. Rev. C **51**, 2310 (1995)
- [11] T. Rijken and V. G. J. Stoks, Phys. Rev. **C59**, 21 (1999)
- [12] R. Machleidt, Adv. Nucl. and Part. Phys. **19**, 189 (1989)
- [13] H. Kim et al., Nucl. Phys. **A662**, 371 (2000)
- [14] M. Batinić, I. Dadić, I. Šlaus, A. Švarc, B. M. K. Nefkens, and T.-S. H. Lee, Physica Scripta **58**, 15 (1998).
- [15] A. M. Green and S. Wycech, Phys. Rev. **C55**, R2167 (1997) Phys. Rev. **C60**, 035208 (1999).
- [16] T. Feuster and U. Mosel, Phys. Rev. **C58**, 457 (1998)
- [17] H. Garcilazo and M. T. Peña, nucl-th/0002056.
- [18] H. Garcilazo and M. T. Peña, Phys. Rev. C **59**, 2389 (1999).

- [19] AGS at Brookhaven National Laboratory: Experiment E890; R. Chrien, private communication.
- [20] J.F. Germond and C. Wilkin, Nucl. Phys. **A518**, 308 (1990)
- [21] M. Gell-Mann, R. Oakes and B. Renner, Phys. Rev. **175**, 2195 (1968)
- [22] M. Kirchbach, D. O. Riska and K. Tsushima, Nucl. Phys. **A542**, 616 (1992)
- [23] I. Towner, Nucl. Phys. **A542**, 631 (1992)
- [24] T.-S. H. Lee and D. O. Riska, Phys. Rev. Lett. **70**, 2237 (1993)
- [25] L. Tiator, C. Bennhold and S. S. Kamalov, "The eta coupling and the  $S_{11}$  resonance in eta photoproduction on the nucleon", Physics with GeV-Particle Beams", H. Machner and K. Sistemich, World Scientific, 112 (1995).
- [26] H. Garcilazo and E. Moya de Guerra, Phys. Rev. C **52**, 49 (1995).
- [27] R. A. Arndt, Z. Li, L. D. Roper, and R. L. Workman, Phys. Rev. D **43**, 2131 (1991).
- [28] J. D. Walecka, *Theoretical Nuclear and Sub-Nuclear Physics*, Oxford University Press, New York, (1995).
- [29] M. Arima, K. Shimizu, K. Yazaki, Nucl. Phys. **A543**, 613 (1992).
- [30] F. Coester and D. O. Riska, Ann. Phys. (N. Y.) **234**, 141 (1994).
- [31] F. Coester and D. O. Riska, Few-Body Systems **25** (1998) 29
- [32] D. O. Riska and G. E. Brown, eprint nucl-th/0005049
- [33] T-S. H. Lee and A. Matsuyama, Phys. Rev. **C36**, 1459 (1987)
- [34] C. Hanhart, K. Nakayama, Phys. Lett. **B454**, 176 (1999).
- [35] N. Kaiser, Proceedings of the 7th Conference *Mesons and Light Nuclei '98*, Edited by J. Adam, P Bydzovsky, J. Dobes, R. Mach, J. Mares, M. Sotona, World Scientific, (1999).

[36] M Lacombe et al., Phys. Rev. **C21**, 861 (1980)

## FIGURES

Figure 1 - Meson-exchange mechanisms that contribute of the reaction  $pp \rightarrow pp\eta$ .

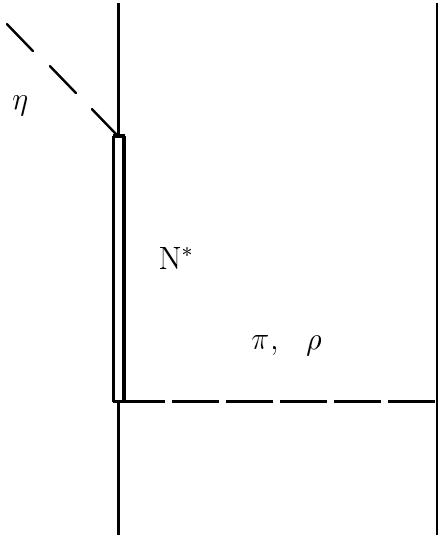
Figure 2 - Diagrammatic representation of the amplitudes that have been considered in this calculation. Figs. 2a, 2b, 2c and 2d are the single nucleon, the  $\eta$  rescattering, the  $\pi$  rescattering and the short-range mechanisms respectively.

Figure 3 - Contribution of the  $\eta$  exchange diagram to the cross-section of the  $pp \rightarrow pp\eta$  reaction. The solid line curve corresponds to a calculation with an off-shell  $\eta N$ - $\eta N$  amplitude with energy dependence and the dash-dot-dotted one to a calculation where the  $\eta N$ - $\eta N$  amplitude strength has its value proportional to the physical scattering length. The short-dashed curve refers to a calculation where the impulse term is added to an  $\eta$ -exchange mechanism built from an off-shell energy dependent  $\eta N \rightarrow \eta N$  amplitude. The data points in this and in the following figures are those given in refs. [2,3].

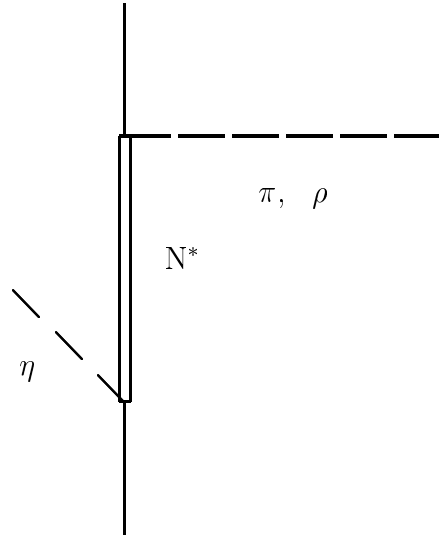
Figure 4 - The contribution of the  $\pi$ -exchange diagram to the cross-section of the  $pp \rightarrow pp\eta$  reaction. The short-dashed curve has the same meaning as in Fig. 3. The dotted-dashed curve includes  $\pi$ -exchange. The full line includes the  $\rho$ -exchange.

Figure 5 - Contribution of the short-range mechanisms to the cross-section of the  $pp \rightarrow pp\eta$  reaction. The short-dashed line has the same meaning as in Figs. 3 and 4, and the short-dot-dashed line refers to a calculation with the impulse+rescattering+short-range amplitudes. The dotted line includes also  $\pi$  exchange and the full line all mechanisms including the  $\rho$ -exchange.

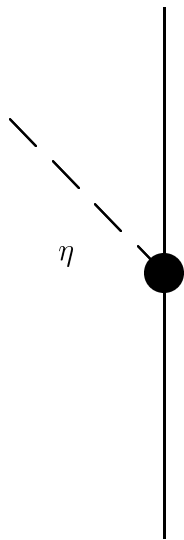
Figure 6 - The calculated total cross-section of the  $pp \rightarrow pp\eta$  reaction as a function of the energy within the models considered in this work. The comparison between the calculations with the Paris (dashed lines) and the Bonn potential (solid lines) for the final state interaction is made. Distinction between the  $\eta N$  amplitude of reference [10] and the one from model A in the second reference of [15] is shown.



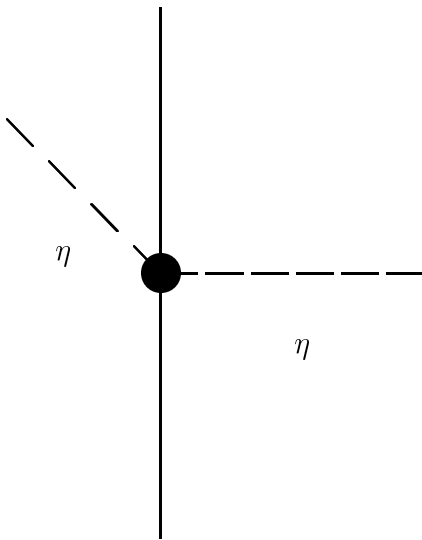
a



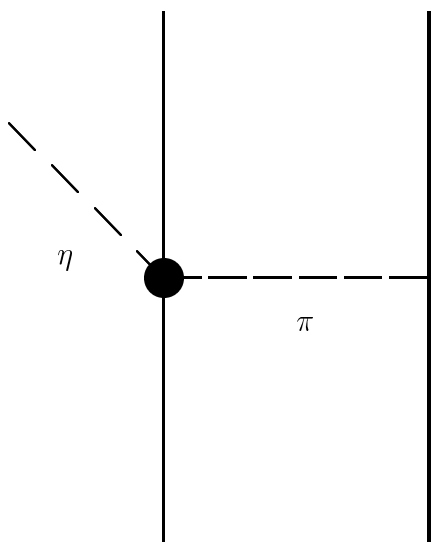
b



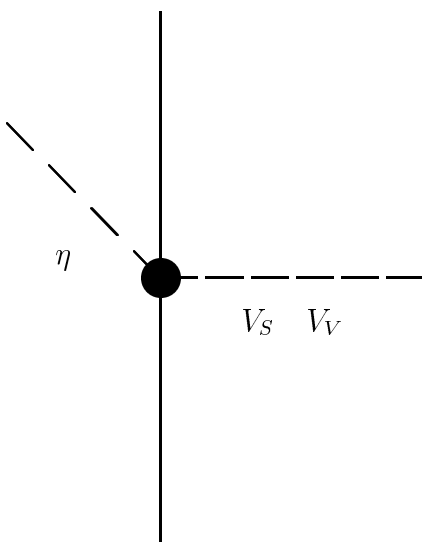
a



b



c



d



